6-12-2019

Interactions of Polyproline II Helix Peptides with Iron(III) Oxide

Charles N. Loney
Case Western Reserve University

Cheyan Xu
Case Western Reserve University

Ashley Graybill
Case Western Reserve University

Julie N. Renner
Case Western Reserve University, jxr484@case.edu

Author(s) ORCID Identifier:

Cheyan Xu

Julie N. Renner

FULL PAPER

Interactions of Polyproline II Helix Peptides with Iron(III) Oxide

Charles N. Loney,[a] Sergio I. Perez Bakovic,[b] Cheyan Xu,[a] Ashley Graybill,[a] Lauren F. Greenlee,[b] and Julie N. Renner[a*]*

Abstract: Interactions of a peptide with polyproline II helical secondary structure with maghemite (iron(III) oxide, Fe_2O_3) surfaces were characterized using a variety of surface techniques. A quartz crystal microbalance with dissipation was used to measure the hydrated mass and thickness (92 ± 29 ng/cm^2 and 0.89 ± 0.27 nm, respectively) of a layer which formed after a sensor coated with Fe_2O_3 was exposed to the peptide in aqueous solution. The analysis revealed that the peptide formed a stable thin layer on the sensor. X-ray photoelectron spectroscopy and Fourier-transform infrared spectroscopy of the monolayer were employed to study the relationship between the metal and the peptide. Finally, Fe_2O_3 nanoparticles were incubated with the peptide, and analysis of the settling and particle size revealed that the presence of the peptide reduced the occurrence of large aggregates in solution.

Introduction

Peptide-metal oxide interactions are important for biomedical and biocatalytic applications, as peptides can affect the surface properties, reactivity, and durability of materials. Iron oxide is a particularly important material because of its potential uses in cancer therapy, macromolecule delivery, and diagnostics via magnetic resonance imaging,[1] in addition to catalytic and electrocatalytic applications for high-impact processes such as ammonia production.[2] Short peptide monolayers are desirable because they form thin layers, are biocompatible, prevent nanoparticle aggregation, and can include multiple functionalities. While various peptide and amino acid systems have been attached to iron oxide,[3] details about the layer, such as mass loading or thickness, are often not reported. Additionally, none of the studies investigate polyproline II (PPII) helices specifically, which are important and prevalent protein structures. Over 400 cell signaling domains recognize proline-rich sequences,[4] where PPII helices are a major structural confirmation. The PPII helical structure is common in globular proteins,[5] with an estimated 10% of individual amino acids in proteins found to be in a PPII helix configuration.[6] PPII helices are unable to make local hydrogen bonds that are characteristic of alpha helices or beta strands, which makes PPII helices more suited for interactions with other molecules and materials.[7]

Because iron oxide nanomaterials are increasingly common in catalytic and biological applications, and because the PPII helix is such a prevalent secondary structure, we aim to study the interaction of a PPII helical peptide with iron oxide materials. Additionally, past work by Nowinski et al. has shown that a proline-rich anchor promotes higher packing densities on gold,[8] and this phenomenon has not been studied on iron oxide. In this study, circular dichroism (CD) is used to confirm the PPII helix secondary structure of the peptides in solution. The assembled layer of a PPII helical peptide is characterized via a quartz crystal microbalance with dissipation (QCM-D), a powerful technique which is used to quantify the peptide hydrated mass and thickness. Furthermore, both X-ray photoelectron spectroscopy (XPS) and Fourier transform infrared spectroscopy (FTIR) are used to explore the modes of binding. Finally, a peptide-functionalized nanomaterial is synthesized with repeatable peptide loading, analyzed for gas adsorption and aggregation behavior, and compared to material without peptide. Overall, the goal of this study is to provide insight into the interactions of PPII helical peptide structures with Fe_2O_3 materials.

Results and Discussion

Peptide Secondary Structure in Solution

The peptide in this work was designed to have high PPII helix propensity and be detectable via fluorescence so that loading could be estimated on nanoparticles. A sequence studied by Brown et al.[9] (GPPLPPGY) was modified with a tryptophan tag such that the final peptide sequence was NH_3-GPPLPPGYGGGGW-COOH (PPII peptide). Circular dichroism (CD) spectra were obtained to determine both the peptide's secondary structure in solution as well as its stability in higher temperature environments. Previous CD spectra taken by Brown et al. showed that the PPII helix sequence without the tryptophan tag had a characteristic positive peak around 225 nm and a negative peak around 202 nm. The positive and negative peaks were interpreted to be representative of a two-state equilibrium between the PPII helix (positive peak) and the disordered state (negative peak).[9] CD analysis in solution confirmed that the designed peptide with an added tryptophan tag had a PPII helix structure, as seen in Fig. 1, which shows a positive and negative band around 225 and 200 nm, respectively. Furthermore, the

[a] Charles N. Loney, Cheyan Xu, Ashley Graybill, and Dr. Julie N. Renner
Department of Chemical and Biomolecular Engineering
Case Western Reserve University, 10900 Euclid Ave.
Cleveland, OH 44106 E-mail: jxr484@case.edu
[b] Sergio I. Perez Bakovic and Dr. Lauren F. Greenlee
Ralph E. Martin Department of Chemical Engineering
University of Arkansas, 4183 Bell Engineering Center,
Fayetteville, AR 72701 E-mail: greenlee@uark.edu

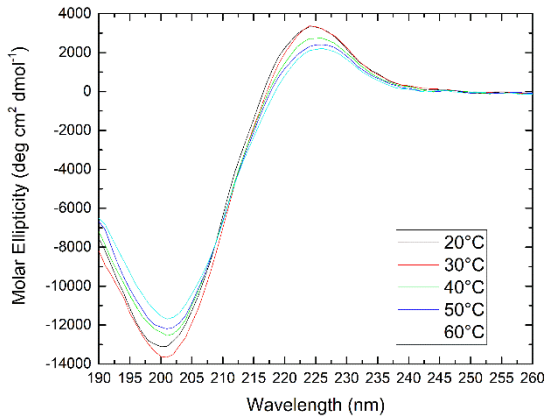

Figure 1. PPII helix peptide with tryptophan tag maintains secondary structure and heat stability up to 60°C. CD spectra of the peptide were taken at 150 µg/mL in DI water at 20°C (black line), 30°C (red line), 40°C (green line), 50°C (dark blue line), and 60°C (light blue line).

PPII helix structure remained stable in temperatures up to 60°C. This was evidenced by the fact that the peak around 225 nm remained positive, which, if the PPII helix structure had been denatured, would have become negative.[10] Collectively, these results indicate that the addition of the tryptophan tag did not significantly alter the PPII helix structure nor its heat stability. It should be noted that CD spectra were also taken with PPII helix-functionalized nanoparticles in DI water (not shown). While the characteristic PPII peaks were present, the ellipticity measurement was an order of magnitude lower due to the light being blocked by the nanoparticles, and it was difficult to differentiate surface-bound signal from the small amount of peptide which may have disassociated into the solution.

Quartz Crystal Microbalance with Dissipation Monitoring Analysis

Binding analysis of the PPII helix peptide to a Fe_2O_3 surface was conducted via QCM-D (Fig. 2). In this technique, a negative relative frequency shift indicates that the surface is gaining hydrated mass, while shifts in dissipation can be used to derive mechanical property information. Fig. 2a shows representative QCM-D data out of 10 total runs. DI water served as the baseline, and after the peptide solution was introduced, the frequency shifted negative, indicating that peptide was bound to the surface. After the surface was rinsed with water, the frequency shifted positive, but stabilized at a value below the original baseline, indicating loosely bound peptide had been rinsed away, leaving a relatively stable layer behind. A prominent feature of these experiments is that there were two distinct slopes, and the DI water rinse stabilized where the first slope ended. This behavior was interpreted such that the first slope was attributed to strong monolayer formation (binding of peptide with Fe_2O_3), and the second slope was attributed to weaker multilayer formation (binding of free peptide with bound peptide). The behavior is similar to other peptide-metal adsorption profiles where two binding events are occurring with different affinities.[11] In addition, the dissipation remained constant, indicating the layer was rigid. Therefore, the Sauerbrey model was used to calculate the

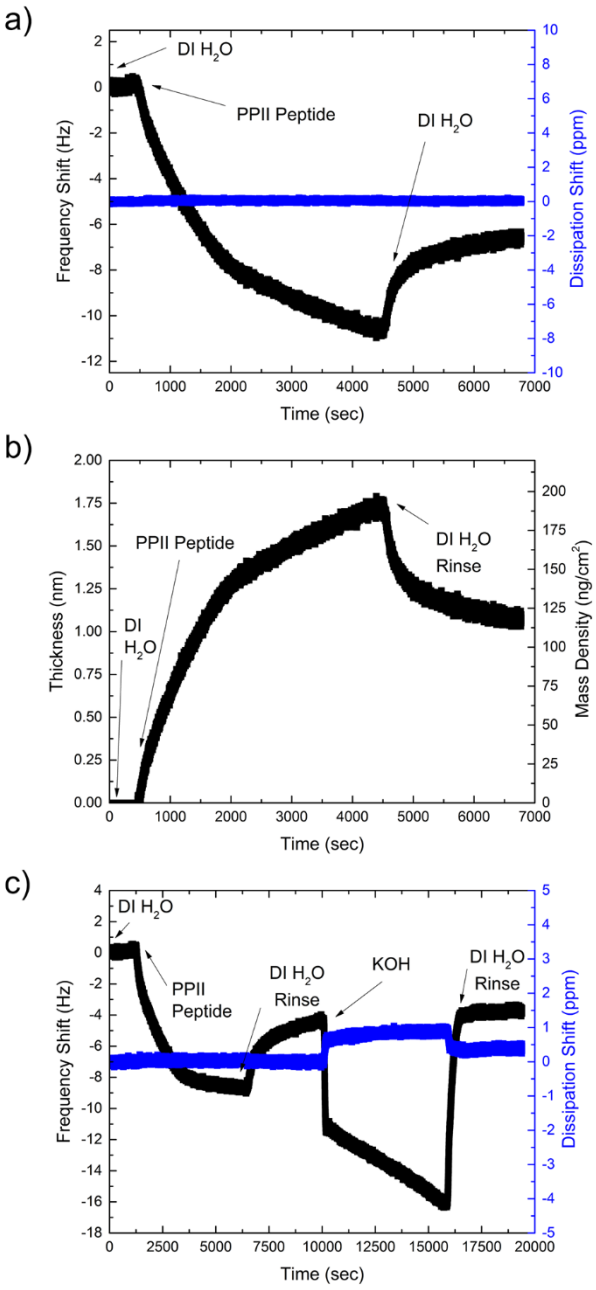

Figure 2. QCM-D monitoring shows that a thin PPII helix peptide layer forms on Fe_2O_3 surfaces. (a) Representative QCM-D frequency (black) and dissipation (blue) monitoring with time. (b) Hydrated thickness and mass density profiles calculated from QCM-D data. (c) Representative QCM-D frequency (black) and dissipation (blue) of a PPII helix peptide monolayer on Fe_2O_3 with a 10 mM KOH rinse (pH 12) step after peptide functionalization to test short-term stability in basic solutions.

hydrated mass.[12] The hydrated density of the protein was assumed to be 1100 g/cm^3 and was used to estimate thickness from the mass data. A description of the QCM equations can be found in Supporting Information along with a summary table of the

10 runs (Table S1). Fig. 2b depicts a time dependent estimate of calculated hydrated peptide mass uptake and thickness, which equilibrated to 92 ± 29 ng/cm^2 and 0.89 ± 0.27 nm, respectively. While PPII helical sequences have been shown to attach to gold,[8, 13] no PPII specific system has been explored on Fe_2O_3. In an attempt to compare these results with literature, one relevant study characterized the range of amino acid attachment to an iron oxide material to be 9-200 ng/cm^2 (estimated from molecules/nm^2, assumed dry mass).[3] The lower end of this range is consistent with our data. We note that the layer formation in our experiments occurred with no change in dissipation, which typically means lower amounts of coupled water.[14]

Peptide stability in basic conditions is relevant to biomedical fields, as blood pH is slightly alkaline. Additionally, it may be desirable to utilize a monolayer in slightly basic catalytic systems. Therefore, to understand if the peptide is stable in these conditions, Fig. 2c shows a QCM-D experiment where a PPII peptide layer was allowed to deposit on a Fe_2O_3 coated sensor in DI water. After a DI water rinse, the sensor was exposed to 10 mM KOH (pH ~12) for a period of ~1.5 hr. After a final DI water rinse, the frequency remained the same as prior to KOH exposure, indicating that the peptide layer was stable short-term under basic conditions.

Surface Analysis of PPII Helix Peptide Monolayers on Fe_2O_3 Surfaces

To characterize the bonds between the Fe_2O_3 surface and the PPII helix peptide, x-ray photoelectron spectroscopy (XPS) was performed. Clean Fe_2O_3 QCM sensors, PPII helix peptide functionalized Fe_2O_3 QCM sensors, and PPII helix peptide powder on a silica wafer were analyzed. Fig. 3a depicts XPS in the N 1s binding energy region, where all surfaces resulted in a peak at ~400 eV. This peak represents the nitrogen in the amide bonds (O=C-N-2R) of the peptide.[15] Bhattacharya et al.[15] reported that peaks are observed at 395.3 eV and 392.4 eV for deprotonated amine groups and Fe-N associations, respectively, of a protein-iron oxide nanocomposite; our results in Fig. 3a show no evidence above the baseline noise of the high resolution scan for peaks at these particular locations. This result suggests that there were no significant interactions between the Fe_2O_3 surface and nitrogen in the peptide.

Generally, the presence of peptide on the Fe_2O_3 and silica surfaces is indicated in the C 1s spectra, with increased carbonyl contribution on peptide-functionalized surfaces as compared to bare Fe_2O_3 (shift in peak position from 288.7 eV to 287.9 eV in Fig. 3b), [15-16] where there are more carboxylic acid contributions because of the likely contaminants. The percent contribution of each fitted peak to the whole spectrum of the C 1s binding energy region, as well as the O 1s region, is summarized in Table 1.

Table 1. Percent contribution of fitted peaks for the C 1s and O 1s binding energy regions of the XPS.

Sample	C1s Peak (eV)	% Contribution	O1s Peak (eV)	% Contribution
Bare Fe_2O_3	284.7 286.2 288.7	62 30 8	529.6 531.1	49 51
Peptide-Functionalized Fe_2O_3	284.8 286.2 288.2	65 18 17	529.6 531.4	54 46
Peptide-Functionalized Silica	284.5 285.8 287.9	43 36 21	532.1	100

XPS of the O 1s range is shown in Fig. 3c and can be used to further study Fe-O interactions. Both the bare and peptide-functionalized Fe_2O_3 surfaces resulted in a peak at 529.6 eV, which is well-supported by literature to result from the Fe-O oxygen chemical environment of iron oxide materials.[15-16, 17] The bare Fe_2O_3 surface also has a shoulder at 531.1 eV, while the peptide-functionalized Fe_2O_3 has a shoulder at 531.4 eV. Yamamoto et al.[18] demonstrated an emergence of a shoulder at +1.8 eV from the Fe-O peak through a series of XPS measurements as a function of pressure. This shoulder was assigned by the authors to oxygen-carbon chemical interactions. An additional shoulder at +1.5 eV from the Fe-O peak was assigned to hydroxyl chemistry.[18] Even under ultra-high vacuum, this peak is observed for Fe_2O_3 materials and has been attributed to non-stoichiometric oxygen or hydroxyl species from minor, residual water molecules associated with the oxide surface.[18]

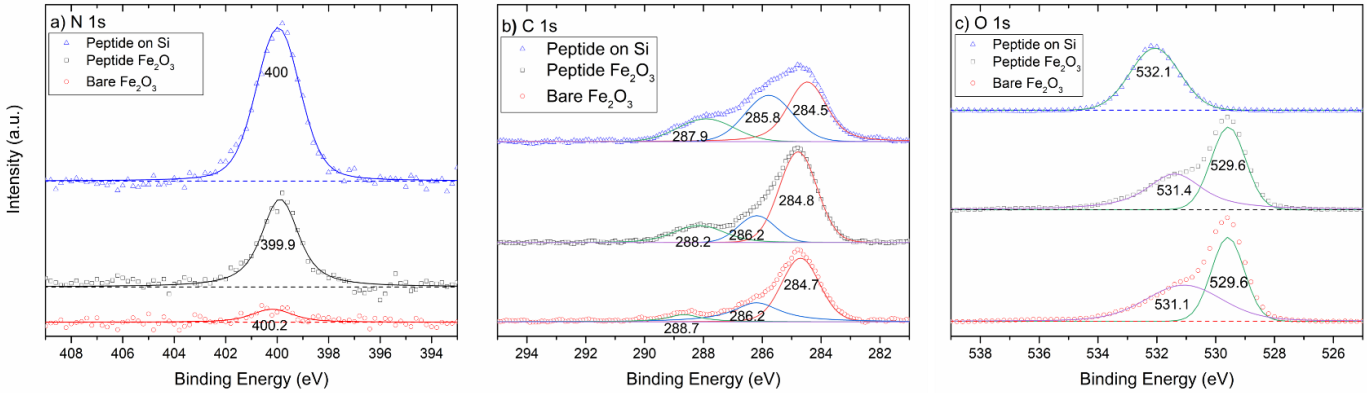

Figure 3. XPS of N1s (a), C1s (b), and O1s (c) ranges with bare PPII peptide (blue triangles), PPII peptide-functionalized Fe_2O_3 (black squares), and bare Fe_2O_3 (red circles).

The similar, subtle shift observed in the data of Fig. 3c, where the O 1s shoulder shifts from 531.1 eV to 531.4 eV, may suggest an interaction of the iron oxide surface with carboxyl and/or carbonyl carbon/carbon-hydroxyl groups of the peptide for the peptide-functionalized Fe_2O_3 surface, as compared to the bare Fe_2O_3 surface, where only hydroxyl contributions would be expected. This analysis is further supported by other studies.[16b, 19] From these results of detailed XPS binding energy regions of C 1s, N 1s, and O 1s, we conclude that there were no apparent Fe-N interactions, and that instead the peptide was interacting with the Fe_2O_3 surface through carbon-oxygen groups.

To supplement the analysis above, background subtracted FTIR spectra of a Fe_2O_3 QCM sensor with PPII helix peptide was taken (Fig. 4) and compared to spectra from peptide powder. In studies with single amino acids, the NH_3^+ symmetric stretch peak (typically found between 1513 cm^{-1} and 1558 cm^{-1}) often disappeared in samples with adsorbed amino acids on magnetite, except in the case of cysteine.[3l] The presence of this peak in the spectra of both samples (1517 cm^{-1}) supports that lack of an interaction between the Fe_2O_3 and the protonated amine. The peak here also suggests the presence of tyrosine.[20] Next, a peak at 1404 cm^{-1} has been previously assigned to Fe_2O_3 interactions with a carboxylate (COO^-) group via 2 O atoms and via a polar covalent bond.[21] The results in this study feature a peak at 1393 cm^{-1} in the peptide-functionalized sample, but not the powder, which strongly suggests such an interaction between the PPII helix peptide and Fe_2O_3. Both samples had a peak at 1639 cm^{-1}, which is assigned to the amide I for PPII helices.[22] The spectra had a peak in the range of 1440-1450 cm^{-1}, which is assigned as amide II, and previous literature has shown PPII helices having dry and aqueous amide II peaks at 1427 and 1456 cm^{-1}, respectively.[22] The peptide layer on Fe_2O_3 also had a peak within this range. The peak at 1335 cm^{-1}, is assigned the CH_2 wagging vibration of proline side chains.[20] Collectively, these results corroborate the XPS results, which also implied binding via carbon-oxygen species and not via NH_3^+. Finally, the broad peaks in the FTIR spectrum generally imply complex interactions are occurring. The results also support that the peptide PPII helix structure is maintained on the surface because it has similarly placed amide I and II peaks, as compared to the neat powder.

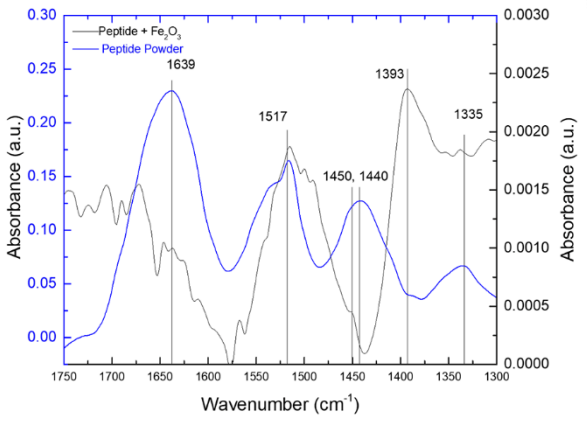

Figure 4. FTIR spectrum of a PPII helix peptide monolayer on an Fe_2O_3 surface (black) compared to neat peptide powder (blue).

Contact angle surface characterization was also performed on the sensors (Fig. S1) and revealed no measurable difference in hydrophobicity between the PPII-functionalized and the bare Fe_2O_3 surfaces.

Preparation and Characterization of Peptide-Functionalized Fe_2O_3 Nanoparticles

Nanoparticles were functionalized with PPII helix peptides using a simple incubation and rinsing protocol. We confirmed with the manufacturer that there was no surface treatment of the material or addition of any surfactant, and thus, it is assumed the nanoparticles are a comparable surface to the QCM-D sensors. The loading of the PPII helix peptide functionalized-Fe_2O_3 nanoparticles was measured via fluorescence readings from a plate reader (calibration shown in Fig. S2). By calculating the peptide in DI water and IPA rinses, peptide that remained on the Fe_2O_3 nanoparticles could be determined via a simple mass balance. The average PPII peptide loading on Fe_2O_3 nanoparticles was 9.6 ± 0.3 mg per each 100 mg of Fe_2O_3. Given that the surface area of Fe_2O_3 reported from the manufacturer was given as 50-245 m^2/g, there were 0.19-0.96 peptides/nm^2 on the nanoparticles. This is comparable to the low end of the range reported in literature for amino acids attached to iron oxide (0.7-5.5 molecules/nm^2),[3l] which is expected considering the peptides are bulkier than single amino acids.

An N_2 gas adsorption isotherm was performed to characterize the effect of peptide functionalization on the relative surface area of the Fe_2O_3 nanoparticles. Fig. S3 shows there was no significant difference between the nitrogen uptake between the functionalized Fe_2O_3 nanoparticles and the bare Fe_2O_3 nanoparticles, indicating that the surface areas were not significantly different from each other.

It was observed that the nanoparticles with the peptide had fewer large agglomerates than the nanoparticles without peptide, shown in Fig. 5a. Samples without peptide were observed to have accumulation of particles visible in the bottom of a cuvette. The prevention of very large aggregates is potentially an attractive property. This behavior was measured quantitatively via dynamic light scattering (DLS), shown in Fig. 5b, which shows the particle size distribution by intensity. Both samples exhibit a population of particles around 100-200 nm, which is close to the manufacturer's specification of 50 nm, and then another population of larger particles. This second population consists of smaller particles in the samples with peptide versus without by approximately an order of magnitude. The DLS analysis studies also investigated the particle size distribution by volume (Fig. S4a), and the results showed a similar trend. When converted to a size distribution by number (Fig. S4b), the data indicated that there were few very large particles in relation to the number of small particles. The peptide appeared to break up or prevent the very large agglomerates (> 1 µm) and produce a wider range of smaller particles. The estimated polydispersity indices of ~30% and 8% for the PPII peptide-functionalized Fe_2O_3 and the bare Fe_2O_3 nanoparticles, respectively, support this analysis.

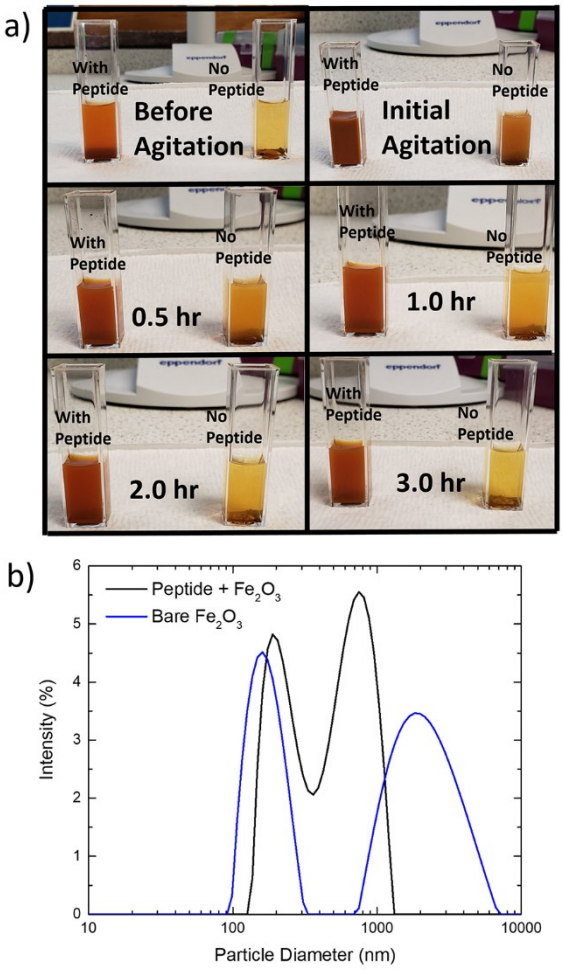

Figure 5. PPII helix peptide-functionalized nanoparticle samples contain less large aggregates. (a) Images of bare Fe_2O_3 nanoparticles and peptide-functionalized nanoparticles in DI water, ranging from initial agitation to 3.0 hr of settling time. (b) Particle size distribution by intensity obtained via DLS to quantify the observation of very large agglomerates (> 1 μm) in bare nanoparticle samples versus the absence of these particles in peptide-functionalized samples.

Furthermore, inspection using scanning electron microscopy (SEM) on Fe_2O_3 nanoparticles (Fig. S5) was conducted to support the claim that the PPII helix peptide prevents Fe_2O_3 agglomerates: SEM depicted a few very large agglomerates in the sample without the PPII helix peptide. It should be noted that direct size comparisons were difficult to make since DLS is conducted in solution, whereas SEM is conducted on a dried sample.

Zeta potential measurements were also conducted to understand the surface charge of the samples. A positive zeta potential of 30-40 mV was measured for the PPII functionalized Fe_2O_3 nanoparticles and the bare Fe_2O_3 nanoparticles. The positive charge of the peptide on the particles in DI water (which is mildly acidic) would be consistent with the XPS and FTIR results indicating that attachment does not occur via protonated amine groups.

Conclusions

Interactions of a PPII helical peptide with Fe_2O_3 materials were characterized, revealing that the peptides formed a thin layer on Fe_2O_3. The layer was stable under basic (pH 12) conditions for at least 1.5 hr. The peptide interacted with the Fe_2O_3 surface through carbon-oxygen groups and not iron-nitrogen, and the polyproline II helix structure was maintained when bound to the surface. In addition, a polyproline II helix peptide-functionalized Fe_2O_3 nanomaterial was synthesized, and it was found that the peptide-functionalized particles had fewer very large agglomerates (> 1 μm) than in samples without the peptide. Overall, our findings give a more detailed understanding of the interactions of polyproline II helix structures with Fe_2O_3, and that understanding was used to create a nanomaterial. In the future, the polyproline II helix-functionalized nanomaterial could serve as an excellent platform for studying the effect of peptide ligands with specific secondary structures on catalysis, could be explored for attractive antifouling behavior, or could be studied under physiological conditions as a biomedical coating.

Supporting Information Summary

Supporting information contains experimental procedures, details about the QCM-D analysis and data from repeated QCM-D runs (Table S1), contact angle measurements of QCM-D samples (Figure S1), calibration curves used to estimate the amount of peptide on functionalized nanoparticles (Figure S2), nitrogen gas adsorption experimental data (Figure S3), nanoparticle size distribution by volume and number from DLS (Figure S4), and SEM images of nanoparticle samples (Figure S5).

Acknowledgements

This work was primarily supported by the U.S. Department of Energy, Office of Science, Basic Energy Sciences, Catalysis Science Program, under Award # DE-SC0016529. CL and SIPB were directly supported by Award DE-SC0016529 to perform the experimental work and analysis for this publication. LFG and JNR were supported by Award DE-SC0016529 during the experimental work and analysis performed for this publication. The initial idea for exploring the PPII helix peptide was conceived during prior support by a U.S. Department of Energy Small Business Innovation Research (SBIR) grant, Grant Number DE-SC0015956, which supported LFG and JNR. We extend our gratitude to both of these programs for helping advance this exciting field. We also thank Smarajit Bandyopadhyay at the Department of Cellular and Molecular Medicine in Cleveland Clinic for his help with CD experiments, the Case Center for Biomolecular Engineering for help with DLS, and the Swagelok Center for Surface Analysis of Materials for help with SEM.

Keywords: • iron(III) oxide • nanoparticles • peptides • polyproline II helix • quartz crystal microbalance with dissipation

References

[1] S. Laurent, J. L. Bridot, L. V. Elst, R. N. Muller, *Future medicinal chemistry* **2010**, *2*, 427-449.

[2] S. L. Foster, S. I. P. Bakovic, R. D. Duda, S. Maheshwari, R. D. Milton, S. D. Minteer, M. J. Janik, J. N. Renner, L. F. Greenlee, *Nature Catalysis* **2018**, *1*, 490-500.

[3] a) N. Hildebrandt, D. Hermsdorf, R. Signorell, S. A. Schmitz, U. Diederichsen, *Arkivoc* **2007**, 79-90; b) L. Josephson, C. H. Tung, A. Moore, R. Weissleder, *Bioconjugate Chem.* **1999**, *10*, 186-191; c) E. Schellenberger, F. Rudloff, C. Warmuth, M. Taupitz, B. Hamm, J. Schnorr, *Bioconjugate Chem.* **2008**, *19*, 2440-2445; d) J. Xie, K. Chen, H. Y. Lee, C. J. Xu, A. R. Hsu, S. Peng, X. Y. Chen, S. H. Sun, *J. Am. Chem. Soc.* **2008**, *130*, 7542-+; e) C. F. Zhang, M. Jugold, E. C. Woenne, T. Lammers, B. Morgenstern, M. M. Mueller, H. Zentgraf, M. Bock, M. Eisenhut, W. Semmler, F. Kiessling, *Cancer Res.* **2007**, *67*, 1555-1562; f) T. Wu, X. Ding, B. Su, A. K. Soodeen-Lalloo, L. Zhang, J. Y. Shi, *Clin. Transl. Oncol.* **2018**, *20*, 599-606; g) Z. Medarova, W. Pham, C. Farrar, V. Petkova, A. Moore, *Nature medicine* **2007**, *13*, 372-377; h) X. Q. Liu, W. J. Song, T. M. Sun, P. Z. Zhang, J. Wang, *Mol. Pharm.* **2011**, *8*, 250-259; i) N. Vinzant, J. L. Scholl, C. M. Wu, T. Kindle, R. Koodali, G. L. Forster, *Front. Neurosci.* **2017**, *11*, 10; j) K. L. Ribeiro, I. A. M. Frias, O. L. Franco, S. C. Dias, A. A. Sousa-Junior, O. N. Silva, A. F. Bakuzis, M. D. L. Oliveira, C. A. S. Andrade, *Colloid Surf. B-Biointerfaces* **2018**, *169*, 72-81; k) H. L. Chee, C. R. R. Gan, M. Ng, L. Low, D. G. Fernig, K. K. Bhakoo, D. Paramelle, *ACS Nano* **2018**, *12*, 6480-6491; l) S. P. Schwaminger, P. F. Garcia, G. K. Merck, F. A. Bodensteiner, S. Heissler, S. Gunther, S. Berensmeier, *J. Phys. Chem. C* **2015**, *119*, 23032-23041; m) M. H. Sousa, J. C. Rubim, P. G. Sobrinho, F. A. Tourinho, *J. Magn. Magn. Mater.* **2001**, *225*, 67-72; n) B. R. White, B. T. Stackhouse, J. A. Holcombe, *J. Hazard. Mater.* **2009**, *161*, 848-853; o) Z. Durmus, H. Kavas, M. S. Toprak, A. Baykal, T. G. Altincekic, A. Aslan, A. Bozkurt, S. Cosgun, *Journal of Alloys and Compounds* **2009**, *484*, 371-376; p) J. Y. Park, E. S. Choi, M. J. Baek, G. H. Lee, *Materials Letters* **2009**, *63*, 379-381; q) H. Qu, H. Ma, W. Zhou, C. J. O'Connor, *Inorg. Chim. Acta* **2012**, *389*, 60-65.

[4] A. Zarrinpar, R. P. Bhattacharyya, W. A. Lim, *Science's STKE : signal transduction knowledge environment* **2003**, *2003*, Re8.

[5] a) A. A. Adzhubei, M. J. E. Sternberg, *J. Mol. Biol.* **1993**, *229*, 472-493; b) B. J. Stapley, T. P. Creamer, *Protein Sci.* **1999**, *8*, 587-595.

[6] N. Sreerama, R. W. Woody, *Biochemistry* **1994**, *33*, 10022-10025.

[7] M. V. Cubellis, F. Caillez, T. L. Blundell, S. C. Lovell, *Proteins* **2005**, *58*, 880-892.

[8] A. K. Nowinski, F. Sun, A. D. White, A. J. Keefe, S. Y. Jiang, *Journal of the American Chemical Society* **2012**, *134*, 6000-6005.

[9] A. M. Brown, N. J. Zondlo, *Biochemistry* **2012**, *51*, 5041-5051.

[10] A. A. Adzhubei, M. J. Sternberg, A. A. Makarov, *J. Mol. Biol.* **2013**, *425*, 2100-2132.

[11] C. Tamerler, E. E. Oren, M. Duman, E. Venkatasubramanian, M. Sarikaya, *Langmuir* **2006**, *22*, 7712-7718.

[12] G. Sauerbrey, *J. Physik* **1959**, *155*, 206-212.

[13] Y. Han, H. Noguchi, K. Sakaguchi, K. Uosaki, *Langmuir* **2011**, *27*, 11951-11957.

[14] M. Edvardsson, S. Svedhem, G. Wang, R. Richter, M. Rodahl, B. Kasemo, *Anal. Chem.* **2009**, *81*, 349-361.

[15] S. Bhattacharya, A. Roychowdhury, D. Das, S. Nayar, *RSC Adv.* **2015**, *5*, 89488-89497.

[16] a) N. A. Zubir, C. Yacou, J. Motuzas, X. Zhang, J. C. Diniz da Costa, *Scientific Reports* **2014**, *4*, 4594; b) K. Song, Y. Lee, M. R. Jo, K. M. Nam, Y.-M. Kang, *Nanotechnology* **2012**, *23*, 505401; c) M. Sanchez-Arenillas, E. Mateo-Marti, *Phys. Chem. Chem. Phys.* **2016**, *18*, 27219-27225.

[17] B. Qu, Y. Sun, L. Liu, C. Li, C. Yu, X. Zhang, Y. Chen, *Scientific Reports* **2017**, *7*, 42772.

[18] S. Yamamoto, T. Kendelewicz, J. T. Newberg, G. Ketteler, D. E. Starr, E. R. Mysak, K. J. Andersson, H. Ogasawara, H. Bluhm, M. Salmeron, G. E. Brown, A. Nilsson, *The Journal of Physical Chemistry C* **2010**, *114*, 2256-2266.

[19] S. Chandrasekaran, S. H. Hur, E. J. Kim, B. Rajagopalan, K. F. Babu, V. Senthilkumar, J. S. Chung, W. M. Choi, Y. S. Kim, *RSC Adv.* **2015**, *5*, 29159-29166.

[20] M. Jackson, *Biochimica et Biophysics Acta* **1995**, *1270*, 1-6.

[21] S. Yu, G. M. Chow, *J. Mater. Chem.* **2004**, *14*, 2781-2786.

[22] N. Wellner, *Biochem. J.* **1996**, *319*.

Entry for the Table of Contents

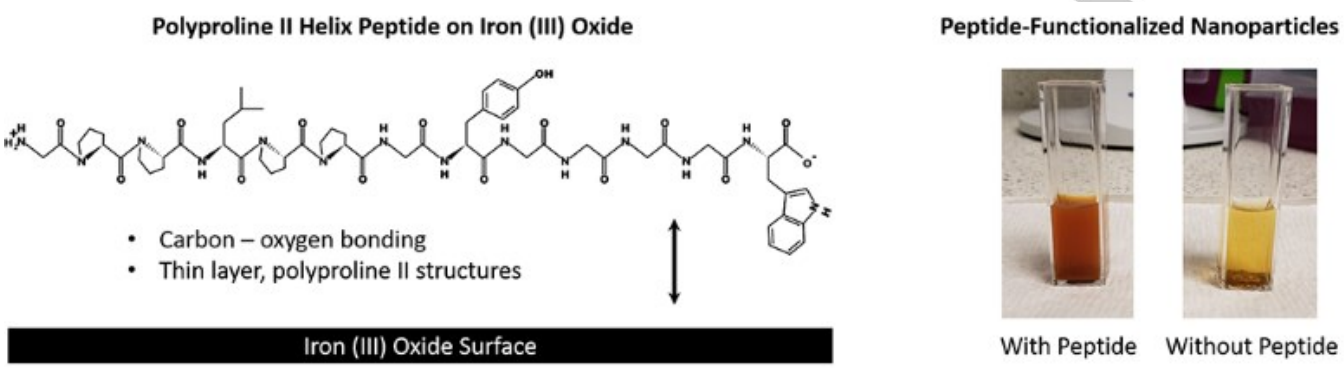

Peptides were found to maintain polyproline II helix structures when attached to iron(III) oxide. The thin peptide layer was formed by interactions with carbon-oxygen groups, and it has an attractive short-term stability in basic pH. Iron(III) oxide nanoparticles functionalized with this new peptide were found to have reduced agglomeration in solution.